

VERTICAL DISTRIBUTION OF OZONE AT THE TERMINATOR ON MARS.

A. Määttänen, F. Lefèvre, S. Guilbon, C. Listowski, F. Montmessin, *LATMOS/IPSL, UVSQ Université Paris-Saclay, UPMC Univ. Paris 06, CNRS, Guyancourt/Paris, France (anni.maattanen@latmos.ipsl.fr).*

Introduction

The SPICAM/Mars Express UV solar occultation dataset gives access to the ozone vertical distribution via the ozone absorption in the Hartley band (220–280 nm). The first results on the ozone vertical distribution from SPICAM were published by [Lebonnois et al. (2006)] using the stellar occultation data. We will present observations of ozone profiles derived from SPICAM solar occultations in the ultraviolet [Määttänen et al. (2013)]. The occultation datasets allow the retrieval of vertical profiles of the abundance of gaseous species, aerosol optical depth and the Ångström coefficient, which can be, through some hypotheses, related to particle size [Montmessin et al. (2006)]. A data analysis code including a correction for mechanical oscillations induced by the MARSIS radar antennae, has been developed [Määttänen et al. (2013)] and was used in the analysis. All solar occultations of adequate quality between orbit numbers 0-10000 (Mars Years 27-30) have been analysed. The dataset spans 4 MY with a good seasonal and spatial coverage. We will present a global overview of the results on the vertical ozone distribution and describe a new method we have developed for comparing the observations to the model.

Dataset

SPICAM (SPectroscopie pour l'Investigation des Caractéristiques Atmosphériques de Mars) has been observing Mars in the ultraviolet (118–320 nm) and in the near infrared (1–1.7 μm) ranges since 2004. Details on the instrument and the observation modes can be found in [Bertaux et al. (2006)]. In the occultation mode, the UV channel gives access to the vertical distribution of CO_2 , O_3 , and aerosols. Here we focus on the UV solar occultation dataset of about 650 profiles. The occultation technique is self-calibrated, since the spectra are normalised with the observed solar spectrum to acquire atmospheric transmissions. The transmission spectra are fitted with the Beer-Lambert law, which takes into account extinction by gaseous species (CO_2 and O_3 in the UV) and aerosols. Aerosol extinction is modeled with the so-called alpha-model, providing access to the Ångström coefficient, which depends on the size of the aerosols. For results on the aerosol vertical distribution see [Määttänen et al. (2013)].

Seasonal behavior of the ozone profiles

Figure 1 displays the climatology of the O_3 profiles derived from the SPICAM solar occultations and the ozone profiles of the Mars General Circulation Model of the Laboratoire de météorologie dynamique (LMD MGCM). Here the comparison is made between local profiles inverted from observations using the onion peeling method and profiles extracted from the model at the grid point nearest to the terminator. The largest ozone amounts are found in spring ($L_s = 20\text{-}50^\circ$) at high northern latitudes ($60^\circ\text{N}\text{-}90^\circ\text{N}$). This result is consistent with the observations of the O_3 column performed by SPICAM in nadir mode [Perrier et al. (2006)] and with the LMD MGCM simulations that predict maximum O_3 amounts in the dry polar vortices in winter and spring [Lefèvre et al. (2008)]. However, our results shed light on the vertical distribution of ozone during that period: we find maximum O_3 densities at about 20 km (note that the high aerosol opacity prevents observations below 10 km) and the top of the O_3 springtime polar layer is located at about 30 km. These altitudes are significantly higher than those simulated by the LMD MGCM, which predicts an O_3 polar layer that is essentially confined below 20 km (right column). This is also the case at southern polar latitudes ($60^\circ\text{S}\text{-}90^\circ\text{S}$), where O_3 is detected by SPICAM solar occultations in autumn and spring above 20 km. This result is consistent with the O_3 profiles derived by stellar occultation at the same time [Lebonnois et al. (2006)]. Both techniques show that more ozone is present above 20 km in the polar vortices than calculated by the LMD MGCM, which suggests that the dehydration in high latitudes extends higher in the real atmosphere than in the model.

At low southern latitudes ($0\text{-}30^\circ\text{S}$), the SPICAM solar occultations show between 30 and 40 km a clear seasonal maximum centred on aphelion ($L_s = 70^\circ$). This result corroborates the nighttime SPICAM measurements by stellar occultation [Lebonnois et al. (2006)] and is also well reproduced by the LMD MGCM (right column). The buildup of this seasonal layer is mainly caused by changes in the vertical distribution of H_2O [Clancy and Nair (1996)]. Around aphelion, the production of hydrogen radicals is much reduced above the low hygropause and so is the ozone loss. In contrast, no ozone is detected by SPICAM at low latitudes in the perihelion season. This can be explained by the dramatic increase in ozone-destroying hydrogen radicals that follow the rise of the hygropause level at that season.

SPICAM ozone vertical distribution

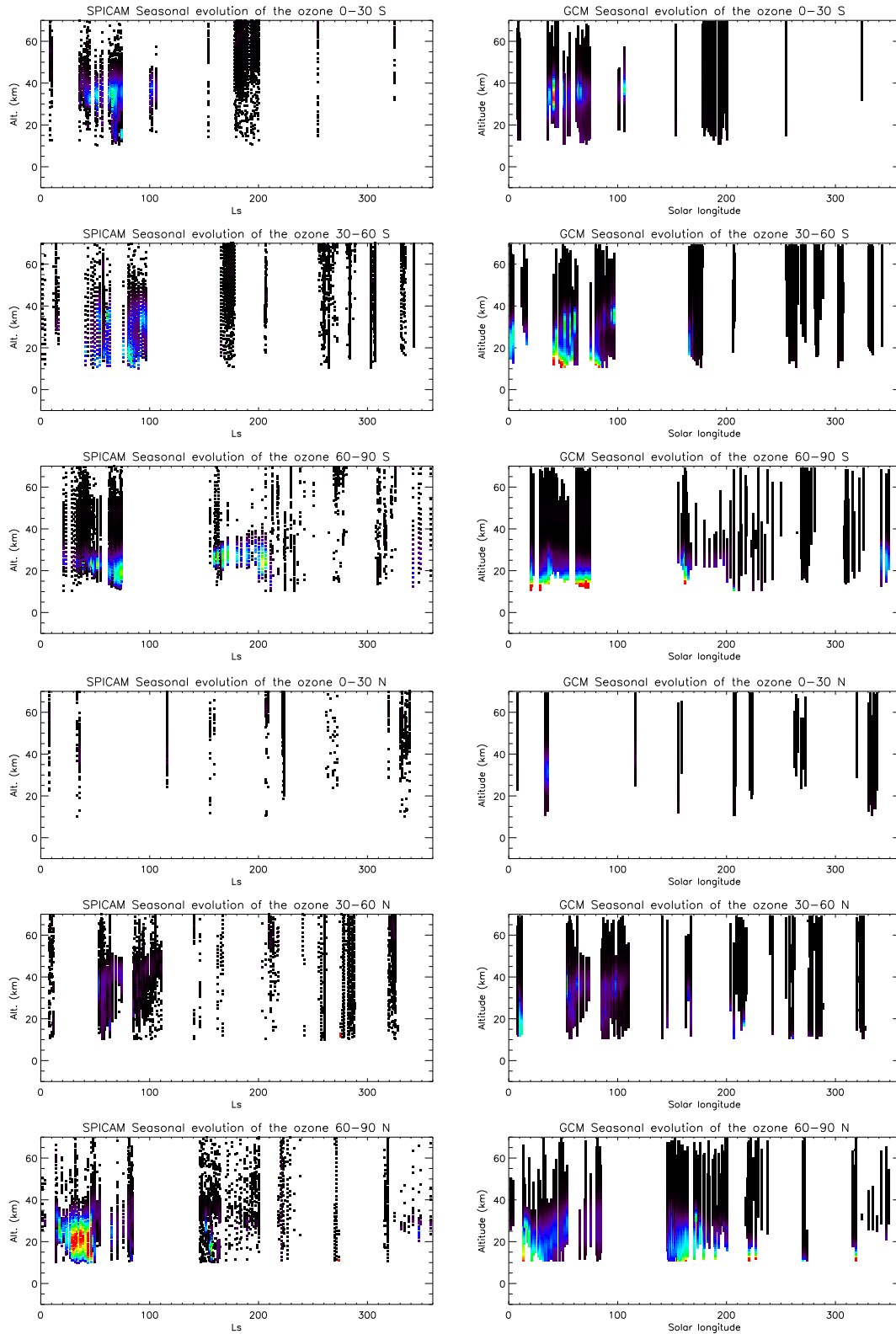


Figure 1: Seasonal evolution of ozone in different latitude bands as observed by SPICAM and modeled by the LMD Mars GCM. The y-axis is altitude between -10 and 70 km above the areoid, the x-axis is the solar longitude, and the color scale goes from 0 to 4×10^9 molecules/m³.

How to compare modeled and observed profiles of a photochemically reactive species at the terminator?

Due to the rapid variation of ozone due to photolysis at sunrise and sunset, a classical comparison of local density profiles is not appropriate for solar occultations that are acquired at the terminator. The spherical symmetry hypothesis made in the onion-peeling vertical inversion method is not valid for photochemically active species (e.g., ozone) around terminator (see Figure 2). Here, we are using a method commonly used in the Earth community. This method exploits the slant profiles (ozone concentration integrated along the line-of-sight of the instrument) for the comparison. For each occultation, we

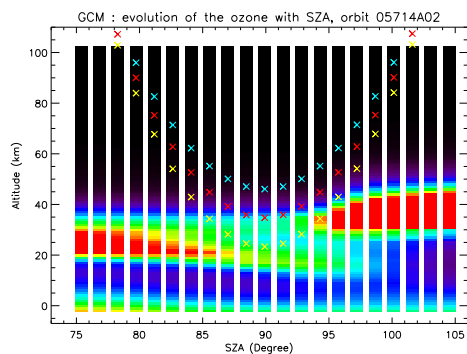


Figure 2: Inhomogeneity of ozone around the terminator and its consequences on the analysis: Modeled ozone profiles (colors) around the terminator during the occultation as a function of the solar zenith angle and examples of three LOS of SPICAM (symbols).

have modeled with the 1D version of the LMD MGCM the ozone vertical and horizontal distribution with high solar zenith angle (or local time) resolution around the terminator (Figure 2). It can be seen that around the terminator the ozone distribution is quite far from spherical symmetry. We then integrate the model results following the lines-of-sight of the occultation (calculated from the observation geometry) to construct the modeled slant profiles (Figure 3).

So far, we have studied six occultations in this manner. In four out of six studied occultations, the slant profile comparison shows quite a good agreement between the model and the observations (for an example, see Figure 3). However, clear differences are seen in some cases, where the observed ozone densities are clearly smaller than the ones extracted from the model (not shown).

We have also tested the possible improvement of the vertical profile comparison by performing the onion-peeling vertical inversion of these slant profiles. The comparison of the model with SPICAM is slightly improved in some cases, but naturally the differences seen in the occultations where SPICAM observes clearly less

ozone than predicted by the model (not shown) persist. In any case, the vertical inversion method we use even for inverting the LOS-integrated model profiles includes the spherical symmetry hypothesis, and thus the comparison of the local profiles is biased.

Thus, the most pertinent comparison is the one between the slant profiles. To completely avoid the problem of the spherical symmetry hypothesis, the inhomogeneity of the atmosphere (for temperature, density/pressure and photochemically active trace gas concentrations) should be fully accounted for within the vertical inversion method. This will be achieved within the UPWARDS project (Work Package lead: BIRA, Belgium).

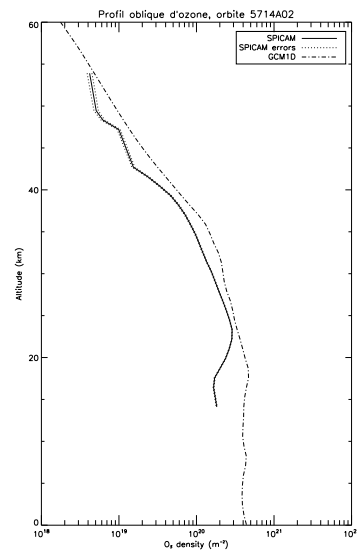


Figure 3: Ozone concentrations integrated along the line-of-sight (slant profiles) from the model (dash-dot line) and the observations (solid line).

Conclusion

We will present a four-year climatology of the ozone vertical distribution on Mars acquired from the analysis of SPICAM UV solar occultations, and we compare it to the modeled climatology. Due to strong spatial variation of ozone across the solar terminator, a classical comparison of local density profiles is not appropriate for solar occultations. We introduce here a method of extracting and comparing the slant profiles also from model results (often used in the Earth community). When the slant profiles are compared, some occultations still present large differences when compared to the model: in two out of six studied cases SPICAM sees a lot less ozone than predicted by the model. For a fully realistic observation-model comparison for photochemical

REFERENCES

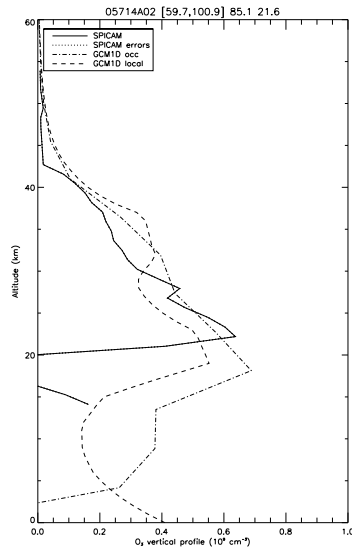


Figure 4: Ozone vertical profiles from SPICAM (solid line) and the model (dash-dot line) after vertical inversion of the slant profiles from Figure 3, and comparison to the modeled local profile at the terminator (dashed line).

species one should compare the slant profiles or account for the heterogeneity of the atmosphere around the terminator in the vertical inversion method (dedicated Work Package in the European project UPWARDS H2020).

Acknowledgements

SPICAM is funded by the French Space Agency CNES and this work has received funding from the European Union's Horizon 2020 Programme (H2020-Compet-08-2014) under grant agreement UPWARDS-633127.

References

[Bertaux et al. (2006)] Bertaux, J., Korablev, O., Perrier, S., Quémerais, E., Montmessin, F., Leblanc, F., Lebonnois, S., Rannou, P., Lefèvre, F., Forget, F., Fedorova, A., Dimarellis, E., Reberac, A., Fonteyn, D., Chaufray, J. Y., Guibert, S., Oct. 2006. SPICAM on Mars Express: Observing modes and overview

of UV spectrometer data and scientific results. *Journal of Geophysical Research (Planets)* 111 (E10), 10–+.

[Clancy and Nair (1996)] Clancy, R. T., Nair, H., 1996. Annual (perihelion-aphelion) cycles in the photochemical behavior of the global Mars atmosphere. *J. Geophys. Res.* 101, 12785–12790.

[Lebonnois et al. (2006)] Lebonnois, S., Quémerais, E., Montmessin, F., Lefevre, F., Perrier, S., Bertaux, J.-L., Forget, F., 2006. Vertical distribution of ozone on Mars as measured by SPICAM/Mars Express using stellar occultation. *Journal of Geophysical Research* 111, E09S05, doi:10.1029/2005JE002643.

[Lefèvre et al. (2008)] Lefèvre, F., Bertaux, J.-L., Clancy, R. T., Encrenaz, T., Fast, K., Forget, F., Lebonnois, S., Montmessin, F., Perrier, S., Aug. 2008. Heterogeneous chemistry in the atmosphere of Mars. *Nature* 454, 971–975.

[Listowski et al. (2011)] Listowski, C., Määttänen, A., Montmessin, F., Lefèvre, F., Bertaux, J.-L., Feb. 2011. Solar Occultation with SPICAM/UV onboard Mars Express: Retrieving Aerosol and Ozone Profiles. In: Forget, F., Millour, E. (Eds.), *Mars Atmosphere: Modelling and observation*. pp. 191–194.

[Määttänen et al. (2013)] Määttänen, A., Listowski, C., Montmessin, F., Maltagliati, L., Reberac, A., Joly, L., Bertaux, J.-L., Apr. 2013. A complete climatology of the aerosol vertical distribution on Mars from MEx/SPICAM UV solar occultations. *Icarus* 223, 892–941.

[Montmessin et al. (2006)] Montmessin, F., Quémerais, E., Bertaux, J.-L., Korablev, O., Rannou, P., Lebonnois, S., 2006. Stellar occultations at UV wavelengths by the SPICAM instrument: Retrieval and analysis of Martian haze profiles. *J. Geophys. Res.* 111, E09S09, doi:10.1029/2005JE002662.

[Perrier et al. (2006)] Perrier, S., Bertaux, J. L., Lefevre, F., Lebonnois, S., Korablev, O., Fedorova, A., Montmessin, F., 2006. Global distribution of total ozone on Mars from SPICAM/MEX UV measurements. *Journal of Geophysical Research* 111, E09S06, doi:10.1029/2006JE002681.